ISSN 1995-0780, Nanotechnologies in Russia, 2020, Vol. 15, Nos. 7–8, pp. 500–506. © Pleiades Publishing, Ltd., 2020.
Russian Text © The Author(s), 2020, published in Rossiiskie Nanotekhnologii, 2020, Vol. 15, No. 4, pp. 532–539.

NANOBIOMEDICINE AND NANOPHARMACEUTICALS

Influence of Synthetic and Native Hydroxyapatite Nanoparticles on the Properties of Mesenchymal Stromal Cells of Bone Marrow

Yu. A. Nashchekina[a,b,*], I. P. Dobrovol'skaya[b,c], E. M. Ivan'kova[b,c], and V. E. Yudin[b,c]

[a] *Institute of Cytology, Russian Academy of Sciences, St. Petersburg, Russia*
[b] *Peter the Great St. Petersburg Polytechnic University, St. Petersburg, Russia*
[c] *Institute of Macromolecular Compounds, Russian Academy of Sciences, St. Petersburg, Russia*
**e-mail: nashchekina.yu@mail.ru*

Received July 2, 2020; revised October 5, 2020; accepted October 6, 2020

Abstract—The synthesis of new forms of hydroxyapatite (HA) and the study of their interaction with living cells are a promising area of modern nanotechnology in chemistry and cell biology. A comparative analysis of the interaction between HA nanoparticles of various origin with living cells is carried out. Scanning electron microscopy revealed that native HA (NHA) particles isolated from native bone tissue are several times larger than that of synthetic HA (SHA) synthesized by a sedimentation method. The pore size and specific surface area of SHA is more than three times larger than similar NHA parameters. The presence of SHA in the culture medium, together with mesenchymal stromal cells, reduces their adhesion, flattening, and proliferation, in contrast to the presence of NHA particles, which have virtually no negative effect on the growth and reproduction of living cells.

10.1134/S1995078020040114

INTRODUCTION

The use of nanoparticles 1–100 nm in size for physical, biomedical, and pharmaceutical tasks is due to their unique physical, chemical, and biological properties [1, 2]. Owing to advances in modern nanotechnology, it has become possible not only to synthesize, but also study the properties of a wide range of nanoscale objects. A promising material for use in regenerative medicine is hydroxyapatite (HA), the properties of which depend on both the composition and size of crystals. HA is a natural mineral form of calcium apatite $Ca_{10}(PO_4)_6(OH)_2$, which, for example, is up to 70 wt % in human bones and teeth. HA has been widely used as a filler to replace amputated bone or as a coating to promote bone ingrowth into prostheses in many surgical areas such as reconstructive surgery [3, 4] and dental implantology [5]. HA is also used to repair early damage to tooth enamel [6].

In addition to bone grafting, due to its high biocompatibility and bioactivity, HA is successfully used in the production of cosmetics and hygiene products. The use of nanosized forms of HA in biomedical fields is constantly increasing due to the high efficiency of gene transfection in drug delivery, as well as good mechanical properties. Note that the physicochemical and structural properties of calcium phosphates strongly depend on their preparation conditions [7–9]. They can be prepared by various methods, such as hydrothermal synthesis, sol–gel synthesis, wet chemical sedimentation, and microwave treatment [10–13]. HA isolated from natural sources has become widely used [14]. Depending on the origin, synthetic or natural, HA has advantages and disadvantages. The small number of comparative studies on the application of HA of various origin to biological objects prevents an unambiguous conclusion and identification of the advantages of a particular method for obtaining HA or raw material sources.

It has been shown in many works that, depending on the physicochemical properties, HA can trigger various biological reactions [15–17]. It was shown that cells and tissues after implantation are influenced not only by the degradation products of HA particles, but also by the particles themselves, as well as their components, which can escape the crystal structure of HA when interacting with the environment. There are data on how the shape, size, or surface charge of HA particles influence cell behavior [18–20].

Despite the combination of unique properties, wide range of synthesis methods, and increase in the number of applications for biomedical problems, the nature of the interaction between HA nanoparticles and cells has not yet been fully investigated [21, 22].

The aim of this study is to comprehensively assess the effect of HA of synthetic and native particles, which have different physicochemical characteristics, on the behavior of mesenchymal stromal cells (MSC) of bone marrow.

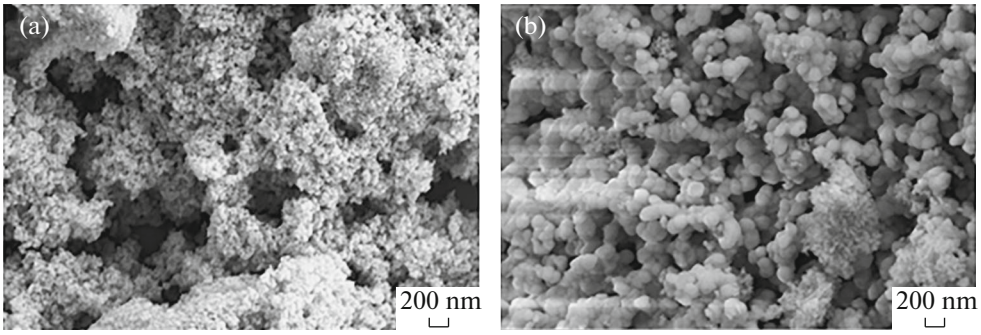

Fig. 1. SEM images of (a) SHA and (b) NHA nanoparticles.

EXPERIMENTAL

Preparation of HA nanoparticles by sedimentation. Synthetic HA nanoparticles (SHA) of calcium were obtained by a sedimentation method from a mixture of phosphoric acid H_3PO_4 and calcium nitrate $Ca(NO_3)_2$ at the Institute of Chemistry, St. Petersburg State University [23].

The pH range (10) and the synthesis temperature (240°C) were determined by the formation of particles with the manifestation of impurity phases and good crystallinity. Magnetic stirrers were used to mix the starting reagents. The resulting mixture was transferred to a 180 mL Teflon autoclave. Then, the closed tank was heated and kept at a predetermined temperature for one hour. The resulting white precipitate was separated by centrifugation (Sigma 2-16P) and washed with distilled water by alternating shaking and collecting steps several times. The finished products were freeze-dried.

Obtaining native HA. Native HA (NHA) [14] was obtained by colleagues from the Institute of Rock Mechanics, from the Laboratory of Composites and Carbon Materials (Prague, Czech Republic). The bones of animals were cut into pieces of required size, and admixtures of bone marrow and soft tissues were removed by heating in a 2% NaCl solution at a pressure of 0.2 MPa and a temperature of 150°C. The resulting pasty mixture was defatted in a solution of acetone and diethyl ether in a volume ratio of 3 : 2 for 24 h. The samples were treated with a 4% NaOH solution at 70°C for 24 h, then the product was annealed at 500°C, atmospheric pressure, and natural humidity to a constant weight. The resulting material was washed with distilled water and heat treated at 105°C.

Bone marrow MSC. The cells were isolated from flat bones of the pelvis of a newborn rabbit, inoculated (1×10^6 cells/cm^2) on Petri dishes, and cultured in αMEM medium (Sigma, USA) containing 10% fetal bovine serum (Gibco, USA) and a mixture of penicillin and streptomycin (Invitrogen, UK), at 5% CO_2 and a temperature of 37°C. Cells of 2–6 passages were used in the experiments.

The Brenauer–Emmett–Taylor method (*BET*). The specific surface area of HA was measured with a NOVA-1200e surface analyzer (USA). Prior to measurements, the matrix was crushed to particles with a size of about 1 mm. A crushed matrix sample weighing at least 200 mg was placed in a cell and degassed for 1.5 h in the appropriate mode. From the difference in the masses of the cell after degassing and the empty cell, the mass of the dried degassed sample was found. Then the cell was placed in a Dewar flask with liquid nitrogen, and the adsorption isotherm was recorded at a pressure of 30 mm Hg.

MTT test. Cell viability was assayed with the MTT test. For the experiment, HA particles with a concentration of 0.3 g/mL were incubated in the αMEM medium for 5 days. The medium with particles was introduced into the wells of a 96-well plate, where MSC were then inoculated (3000 per well), followed by the addition of 10% fetal bovine serum. Cells cultured in a growth medium with serum without HA particles were used as the control. The number of viable cells was assessed after staining of MSC with an MTT solution (3-(4,5-dimethylthiazol-2-yl)-2,5-diphenyltetrazolium bromide) (Sigma, USA). MTT was dissolved in αMEM medium to a final concentration of 5 mg/mL, added to the well, and left for 2 h. After 2 h of exposure at 5% CO_2 and a temperature of 37°C, living cells reduced the yellow MTT to dark purple formazan granules. Formazan granules were dissolved with dimethyl sulfoxide (Sigma, United States), and the optical density of the solution was measured on an enzyme immunoassay analyzer (Fluorophot, Probanauchpribor, Russia) at a wavelength of 570 nm.

Laser scanning microscopy. To assess the morphology of cells in the presence of HA, MSC were stained with rhodamine-phalloidin to reveal the actin cytoskeleton. HA particles at a concentration of 0.3 g/mL were preincubated in αMEM medium for 5 days. Then the growth medium with HA particles was introduced into a Petri dish with a coverslip, on which MSC (10000) were inoculated and 10% fetal bovine serum was added. Cells cultured in a growth medium

Table 1. Specific surface area and porosity of HA particles

HA	Pore volume, cm^3/g	Specific surface, m^2/g
Synthetic	0.19	69.3
Native	0.05	13.6

with serum without HA particles were used as the control. After 1 day of cultivation, nonadherent cells were removed; the adherent MSC were washed with PBS solution (Biolot, Russia) and fixed in 4% formalin solution (Sigma, USA), followed by addition of a 0.1% solution of Triton X-100 (Sigma, USA) and a solution of rhodamine phalloidin (10 U/mL) (Invitrogen, UK). After each treatment, the preparations were washed three times with PBS. Nuclei were stained with DAPI (Invitrogen, UK). Actin filaments were visualized with a scanning laser confocal microscope (LSM 5 Pascal, Germany).

Scanning electron microscopy. Cell morphology after 7 days of cultivation was assessed by scanning electron microscopy (SEM). Samples were fixed with 1% glutaraldehyde solution followed by treatment with ethyl alcohol solution. After fixation, a thin platinum layer was deposited on the samples and examined with a SUPRA 55VP scanning electron microscope (Carl Zeiss).

Statistical processing of results. Statistical processing of results obtained in five replicates were processed in Microsoft Excel 2007, with determination of the mean and standard error. To compare the results, we used Student's *t*-test. The differences were considered significant when $p < 0.05$.

RESULTS

Structural properties of HA nanoparticles. When analyzing SEM images, it can be concluded that the NHA sizes vary over a wide range, from tens of to several hundred nanometers. Figure 1 clearly shows that, in contrast to SHA, NHA assembles into conglomerates and the fraction of conglomerates is much higher than that of nanoparticles, the size of which does not exceed several nanometers. Also, these conglomerates have a dense structure, in contrast to the loose porous

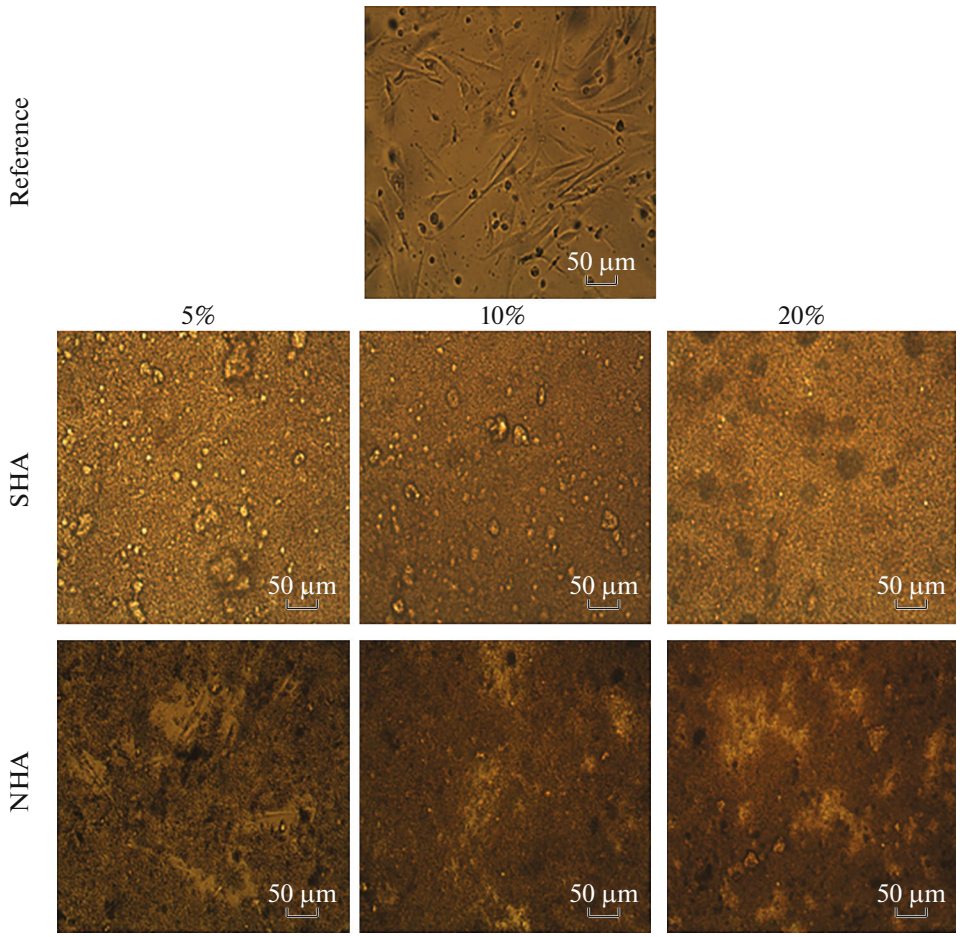

Fig. 2. (Color online) Micrographs of MSC in presence of HA nanoparticles after 1 day of cultivation; 5, 10, and 20%, concentration of HA particles in nutrient medium.

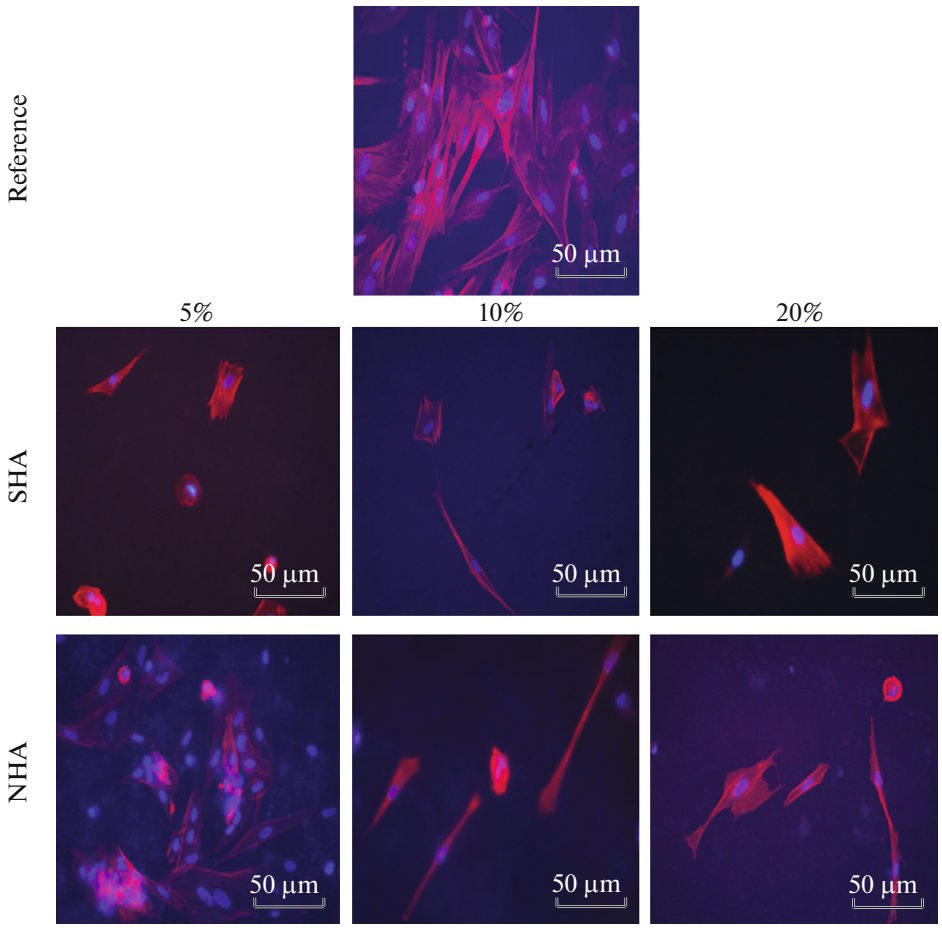

Fig. 3. (Color online) Organization of actin cytoskeleton of MSC after 1 day of cultivation in presence of HA particles (rhodamine-phalloidin staining, red; DAPI, blue); 5, 10, and 20% refer to the concentration of HA particles in the culture medium.

structure of SHA, which consists of nanoparticles no larger than 10 nm.

The BET method was used to determine the specific surface area and porosity of HA particles, shown in Table 1. It can be seen from the table that the specific surface area and pore volume occupied by SHA nanoparticles are more than three times higher than those for NHA nanoparticles.

Optical microscopy. An important parameter influencing the properties of cells, including their morphology, is the amount of HA nanoparticles interacting with cells or the concentration of nanoparticles in the culture medium. To assay the effect of the nanoparticle concentration on MSC, different amounts of HA nanoparticles—5, 10, and 20%—were introduced into the culture medium simultaneously with the inoculation of cells. One day after inoculation, MSC in the control sample have an elongated fusiform shape typical of this type of cells (Fig. 2). When different amounts of SHA nanoparticles are added to the culture medium, the entire surface of the culture dish is evenly covered with particles. Regardless of the particle concentration in an inverted optical microscope, the presence of cells was not observed, which indicates that either all cells are coated with SHA nanoparticles or when a suspension of MSC and SHA nanoparticles is simultaneously added to the culture dish, the cells do not adhere to the surface of the culture dish.

With the simultaneous introduction of MSC and NHA nanoparticles into the culture dish, optical microscopy reveals adhered and flattened spindle-shaped cells among the settled NHA particles. Note that, at all three NHA concentrations, cells are seen among the settled particles (bright fields) in an inverted microscope. In samples with 5% NHA, the spindlelike structure of MSC can be estimated (Fig. 2).

Laser scanning microscopy. To assess the morphological features of MSC cultured in the presence of HA nanoparticles, the nutrient medium together with the particles was removed, and the cells were fixed and stained with a fluorescent dye. Figure 3 shows the results of laser scanning microscopy. After 1 day of cultivation, the cells in the control sample are well flattened. Figure 3 shows well-formed actin filaments

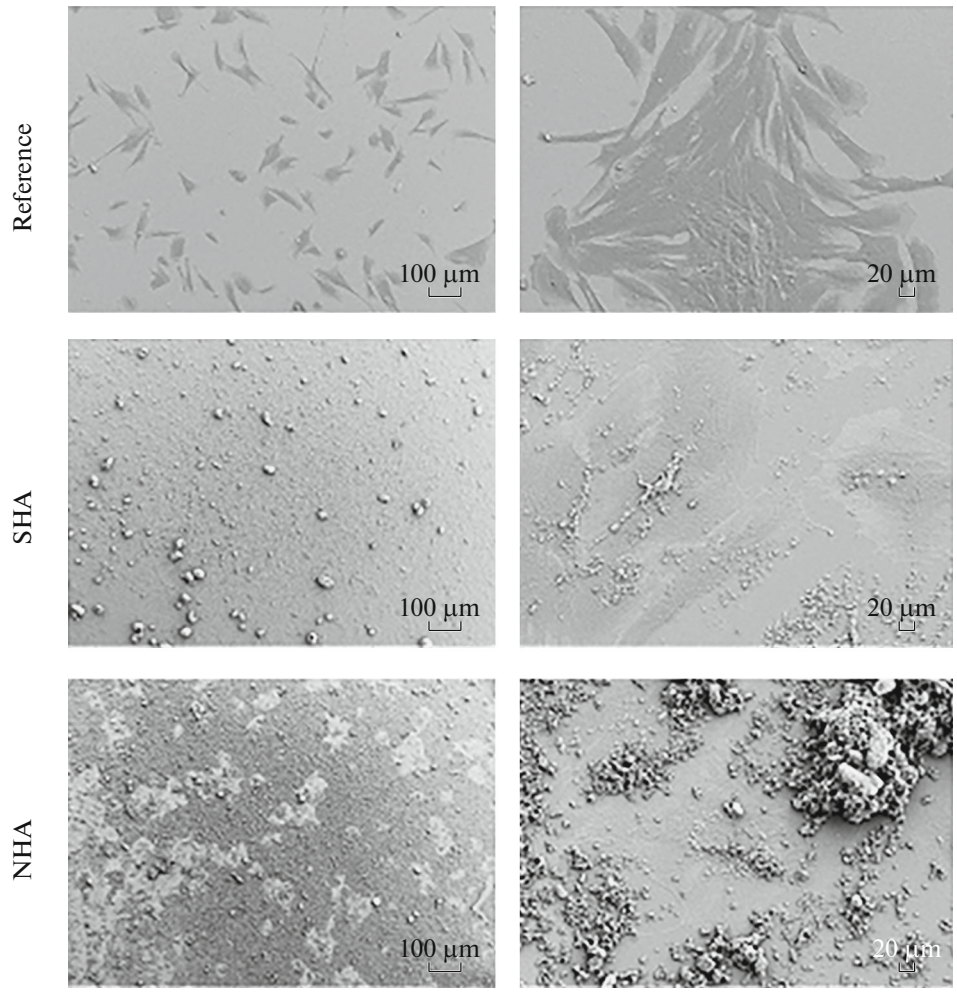

Fig. 4. SEM images of MSC after 1 day of cultivation in presence of 5% HA particles.

over the entire area of the flattened cell. In the presence of SHA, the number of adherent cells 1 day after inoculation is significantly inferior to the control. Only a few cells are visible in the microscope's field of view. The degree of flattening of these cells is also inferior to the control; the cells are mostly rounded and actin is concentrated in the nucleus region. When describing cells cultured in the presence of NHA, a fairly large number of well-flattened MSC on the surface of the culture dish in the presence of 5% NHA were observed. The appearance of cells and their number in this sample does not differ from the control sample—without HA nanoparticles. With an increase in the concentration of NHA in the culture medium to 10%, the number of cells adhering to the culture plastic significantly decreases. In the field of view, only a few cells were observed with a fusiform shape typical of this type of cells, in contrast to cells cultured in the presence of the same amount of SHA. With an increase in the SHA concentration in the culture medium to 20%, the number of adhered cells and their morphology are similar to cells cultured in the presence of 10% SHA (Fig. 3).

Scanning electron microscopy. Direct contact of cells with HA particles was assessed by SEM (Fig. 4). After 1 day of cultivation, the culture medium was removed and the cells were fixed. The SEM data confirm the results obtained by optical and confocal microscopy. When cells were cocultured with SHA at low magnification, complete coverage of SHA over the entire surface of the plate was observed. Note that SHA also partially collect in conglomerates, as evidenced by particles with sizes reaching several tens of microns. For cocultivation of MSC with NHA, the surface of the dish was visualized by SEM, which was discretely covered with particles. Moreover, the areas not covered with particles are occupied by spread cells. A more detailed study of adhered and spread cells revealed MSC coated with HA particles of both natural and synthetic origin. In the presence of NHA, the cells are covered with large conglomerates, and when SHA is added, the cells are covered with smaller particles.

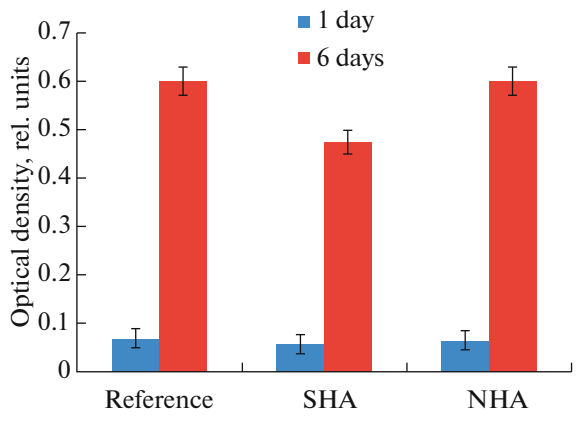

Fig. 5. (Color online) Results of MTT test of MSC after 1 and 6 days of cultivation in presence of 5% HA particles.

MTT analysis. A quantitative assessment of the viability of MSC cultured in the presence of HA particles was performed using MTT analysis. After 1 and 6 days of cultivation, the cells were treated with MTT solution. Formazan formed in living cells was determined spectrophotometrically. Figure 5 shows that the presence of HA nanoparticles in the culture medium insignificantly decreases the ability of MSC to adhere to the culture plastic. With further cultivation, a slight cytotoxic effect of SHA on the cultured cells was observed. After 6 days of cultivation, the number of cells in the presence of SHA is inferior to the number of cells in the control sample. The proliferation of MSC in the presence of NHA does not differ from the control.

DISCUSSION

The chemical composition and crystal structure of HA nanoparticles are similar to the microstructure of natural bones and teeth [24, 25]. It is the structure of HA that imparts particular biological characteristics, such as nonimmunogenicity, good biocompatibility, high osteoconductivity, and osteoinduction [26–28]. Numerous studies have demonstrated the excellent biocompatibility of HA with various cell cultures. Results of the effect of nanoparticle size on cell adhesion and proliferation are presented in [29, 30]. However, as the present study shows, not only the structural characteristics and sizes of nanoparticles affect the cultured cells, but also the cocultivation of cells and HA particles, as well as the origin of the particles.

The results obtained with direct diagnostic methods—electron, optical, and confocal microscopy—demonstrate an identical dependence of cell behavior on the type of HA. When MSC are cultured in the presence of SHA, the particles completely cover the plate surface together with the cells. When MSC are added to a dish together with NHA, a discrete distribution of particles over the surface of the dish is observed. Even with an inverted microscope, it is possible to fix flattened cells between NHA particles. The results obtained can be explained by two processes. The first reason for the discrete distribution of NHA on the surface of the culture dish is associated with the intense interaction of MSC with NHA particles. The cells actively separate the NHA particles that settle from the nutrient medium onto the surface of the culture vessel. At the same time, such a pattern is not observed in dishes with SHA, which may explain the absence of any interaction of cells with SHA. The second assumption is the different sedimentation rates of particles of different origin and the ratio of this rate to that of cell sedimentation. Apparently, this mechanism most objectively describes the results obtained. With the simultaneous inoculation of cells and SHA, cells are the first to settle on the surface of the culture dish, and SHA nanoparticles cover the cells after they flatten. Therefore, using optical and scanning electron microscopy, only the surface of the culture dish can be observed, which is completely covered with particles.

With the simultaneous introduction of MSC and NHA into the culture dish, the heavier particles of NHA are the first to settle onto the surface of the dish and the cells settling behind them are able to move apart the NHA particles. The different sedimentation rates of particles obtained from different sources confirm the BET and SEM data. The specific surface area and pore volume for SHA are more than three times smaller than for similar parameters for NHA. The larger the specific surface area of the particles and pore volume, the lower the density; therefore, lighter particles have a lower sedimentation rate. Obviously, this sedimentation rate is less than that of the cells themselves. These assumptions require further research. Based on the results obtained, it can be concluded that in the presence of NHA, the number of viable cells is greater than that of MSC cultured together with SHA.

FUNDING

The study was financed by the Russian Science Foundation (project no. 19-73-30003).

REFERENCES

1. H. Zhou and J. Lee, Acta Biomater. **7**, 2769 (2011). https://doi.org/10.1016/j.actbio.2011.03.019
2. L. Chen, J. M. Mccrate, J. C.-M. Lee, and H. Li, Nanotechnology **22**, 105708 (2011). https://doi.org/10.1088/0957-4484/22/10/105708
3. A. Matsumine, K. Kusuzaki, T. Matsubara, et al., J. Surg. Oncol. **93**, 212 (2006). https://doi.org/10.1002/jso.20355
4. S. V. Dorozhkin and M. Epple, Angew. Chem. Int. Ed. Eng. **41**, 3130 (2002). https://doi.org/10.1002/1521-3773(20020902)

5. L. John, M. Janeta, and S. Szafert, Mater. Sci. Eng. C **78**, 901 (2017). https://doi.org/10.1016/j.msec.2017.04.133
6. P. A. Brunton, R. P. Davies, J. L. Burke, et al., Br. Dent. J. **215**, E6 (2013). https://doi.org/10.1038/sj
7. M. Okada and T. Furuzono, Sci. Technol. Adv. Mater. **13**, 064103 (2012). https://doi.org/10.1088/1468-6996/13/6/064103
8. X.-Y. Zhao, Y.-J. Zhu, F. Chen, et al., Cryst. Eng. Commun. **15**, 7926 (2013). https://doi.org/10.1039/C3CE41255E
9. M. Kolodziejczyk, D. Smolen, T. Chudoba, et al., Tissue Eng. Regener. Med. **8**, 235 (2014).
10. M. Bilton, S. J. Milne, and A. P. Brown, J. Inorg. Non-Met. Mater. **2**, 1 (2012). https://doi.org/10.4236/ojinm.2012.21001
11. S. S. A. Abidi and Q. J. Murtaza, Mater. Sci. Technol. **30**, 307 (2014). https://doi.org/10.1016/j.jmst.2013.10.011
12. D. Smolen, T. Chudoba, I. Malka, et al., Int. J. Nanomed. **8**, 653 (2013). https://doi.org/10.2147/ijn.s39299
13. A. K. Nayak, Int. J. Chem. Technol. Res. **2**, 903 (2010).
14. M. Šupová, J. Nanosci. Nanotechnol. **14**, 1 (2014). https://doi.org/10.1166/jnn.2014.8895
15. X. Zhao, S. Ng, B. C. Heng, et al., J. Arch. Toxicol. **87**, 1037 (2013). https://doi.org/10.1007/s00204-012-0827-1
16. M. R. Wiesner, G. V. Lowry, P. Alvarez, et al., Environ. Sci. Technol. **40**, 4336 (2006). https://doi.org/10.1021/es062726m
17. A. D. Maynard, R. J. Aitken, T. Butz, et al., Nature (London, U.K.) **444**, 267 (2006). https://doi.org/10.1038/444267
18. M. Motskin, D. M. Wright, K. Muller, et al., Biomaterials **30**, 3307 (2009). https://doi.org/10.1016/j.biomaterials.2009.02.044
19. L. Chen, J. M. Mccrate, J. C.-M. Lee, and H. Li, Nanotechnology **22**, 105708 (2011). https://doi.org/10.1088/0957-4484/22/10/105708
20. Yu. A. Nashchekina, A. S. Chabina, O. M. Osmolovskaya, et al., Tsitologiya, No. 10, 813 (2018).
21. J. Idaszek, E. Kijeńska, M. Łojkowski, and W. Swieszkowski, Appl. Surf. Sci. **388**, 762 (2016). https://doi.org/10.1016/j.apsusc.2016.03.038
22. E. Kijeńska, S. Zhang, M. P. Prabhakaran, et al., Int. J. Polym. Mater. Polym. Biomater. **65**, 807 (2016). https://doi.org/10.1080/00914037.2016.1163561
23. I. P. Dobrovol'skaya, N. S. Tsarev, O. M. Osmolovskaya, I. A. Kasatkin, E. M. Ivan'kova, E. N. Popova, G. A. Pankova, and V. E. Yudin, Russ. J. Appl. Chem. **91**, 368 (2018).
24. T. J. Webster, C. Ergun, R. H. Doremus, et al., Biomaterials **22**, 1327 (2001). https://doi.org/10.1016/s0142-9612(00)00285-4
25. L. L. Hench and J. M. Polak, Science (Washington, DC, U. S.) **295**, 1014 (2002). https://doi.org/10.1126/science.1067404
26. Y. Cai, Y. Liu, W. Yan, et al., J. Mater. Chem. **17**, 3780 (2007).
27. S. J. Kalita, A. Bhardwaj, and H. A. Bhatt, Mater. Sci. Eng. C **27**, 441 (2007).
28. N. Tran and T. J. Webster, Acta Biomater. **7**, 1298 (2011). https://doi.org/10.1016/j.actbio.2010.10.004
29. M. S. Laranjeira, M. H. Fernandes, and F. J. Monteiro, J. Biomed. Mater. Res. A **95**, 891 (2010). https://doi.org/10.1002/jbm.a.32916
30. L. Chen, J. M. Mccrate, J. C. M. Lee, and H. Li, Nanotechnology **22**, 105708 (2011). https://doi.org/10.1088/0957-4484/22/10/105708